In situ peeling of one-dimensional nanostructures using a dual-probe nanotweezer

Hui Xie[a] and Stéphane Régnier
Institut des Systèmes Intelligents et Robotique, Université Pierre et Marie Curie/CNRS UMR 7222, BC 173, 4 Place Jussieu, 75005 Paris, France

(Received 17 January 2010; accepted 20 February 2010; published online 29 March 2010)

We reported a method for *in situ* peeling force measurement of one-dimensional nanostructures using a dual-probe nanotweezer, which is developed on the principle of force microscopy. Benefiting from capabilities of image scanning and accurate force sensing, the nanotweezer is capable of positioning one-dimensional nanostructures deposited on a surface and then performing *in situ* peeling tests with pick-and-place operations at different peeling locations of interest along a selected nanostructure. In experiments, nanoscale peeling of silicon nanowires (SiNWs) on a silicon substrate has been studied. Peeling locations at the end and in the middle of the SiNW were tested and the results indicate that approximate peeling energies are needed. © *2010 American Institute of Physics.* [doi:10.1063/1.3360936]

I. INTRODUCTION

Peeling force measurement at the nanoscale is clearly of interest and is crucial for measuring adhesive strength of micro- and nanoscopic bonding of nanostructures,[1] e.g., interfacial energy measurement for reinforcement of composite materials,[2–5] bionanotechnology characterization,[5–7] and fabrication of nanostructures and nanodevices.[8–15] The peeling test of nanostructures is thus a necessity to understand interfacial phenomena at the nanoscale contact.

Unfortunately, it is generally hard to perform a nanoscale mechanical peeling test, which requires facilities with capabilities to locate, manipulate, and displace nanostructures with nanoscale precision (approximately nanometers) while sensing extremely small peeling forces (approximately nanonewtons). As a uniquely suitable facility capable of nanoscale surface imaging and ultrasmall force sensing, the conventional atomic force microscope (AFM) in the past two decades has succeeded in manipulating nanoparticles,[16–18] single molecules,[19] nanorods,[20] and nanotubes[21] by typical used in-plane pushing or pulling manipulation. However, the nanoscale peeling force measurement, which typically requires out-of-plane manipulation, is still a challenge. Up to now, a few nanoscale peeling researches have been carried out. For instance, nanoscale peeling methods were developed to successfully peel multiwalled carbon nanotubes (MWCNTs) attached to the end of a tipless microcantilever[1] in an AFM or the tip of a self-detective microcantilever[22] integrated in a scanning electron microscope that enables a so-called visualized nanoscale peeling process. The current methods might require strenuous labors of sample preparations by sorting straight MWCNTs out and then attaching them on the microcantilevers. An effective peeling tool is thus necessarily to be developed to facilitate the nanoscale peeling tests.

In this work, we present a new method for *in situ* nanoscale peeling of one-dimensional (1D) nanostructures using a dual-probe nanotweezer, which is modified from our previous work of a parallel imaging/manipulation force microscope.[23] The system is equipped with two independently actuated and sensed microcantilevers with protruding tips that are in opposition to each other, forming a nanotweezer through coordination control. Due to the capability of nanoscale pick-and-place manipulation with accurate force sensing, the nanotweezer is suitable for *in situ* peeling of 1D nanostructures without complicated sample preparation, e.g., single molecules, nanowires, and nanotubes.

II. METHODS

The nanotweezer is formed by two force modulation microcantilevers (NANOSENSORS ATEC-FM, with a nominal stiffness of 2.8 N/m). Forces on each cantilever are independently detected by its own optical lever, which is typically composed of a laser and a quartered photodiode. The calibrated[24] open-loop *X-Y-Z* piezotube (PI P-153.10H) in this configuration is removed from the system base and then fixed on the closed-loop *X-Y-Z* nanostage (MCL Nano-Bio2M on the *X*- and *Y*-axes, and PI P-732.ZC on the *Z*-axis) to form a dual-driven nanopositioning stage. This stage can be used for image scanning, nanotweezer aligning, and nanosamples handling with an especially developed control system. The left microcantilever (probe I) is fixed to the base, while the right microcantilever (probe II) is actuated by the nanostage. The proposed dual-probe nanotweezer is capable of the nanoscale peeling, thanks to the following.

(i) In comparison with the normal diameter of 1D nanostructures to be peeled, the tip apex of the probe is very tiny (typically with an apex radius of 10 nm or less), which leads to a geometrical condition for grasping at the nanoscale as well as smaller adhesive

[a]Author to whom correspondence should be addressed. Electronic mail: xie@isir.upmc.fr.

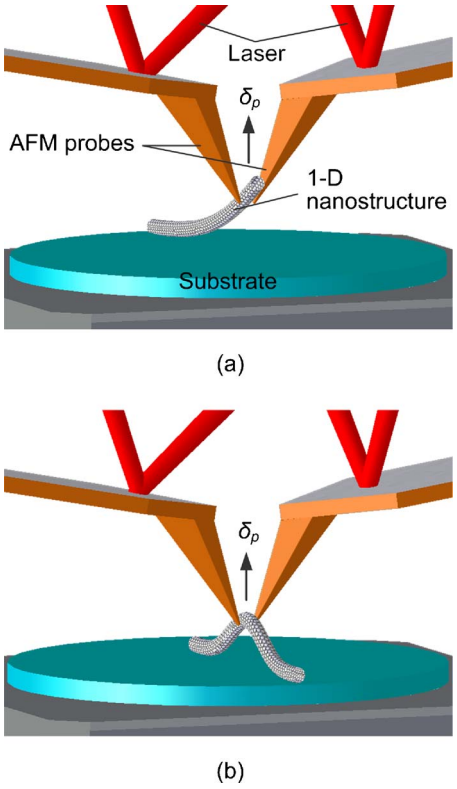

FIG. 1. (Color online) A schematic diagram of a 1D nanostructure peeling force measurement using the dual-probe nanotweezer. (a) Peeling occurs at the end of the 1D nanostructure. (b) Peeling occurs in the middle of the 1D nanostructure. δ_p is the gap between the substrate and the peeling location on the 1D nanostructure. The peeling process is performed by moving the piezotube on the *Z*-axis, while the nanotweezer is fixed. The peeling force is synthesized from bending forces on both cantilevers that are individually detected by their own optical levers.

forces between the nanotweezer and the 1D nanostructures that favor the release process.

(ii) More importantly, the nanotweezer can be used as a normal AFM to image the 1D nanostructures, as well as locate the probes for tweezer alignment. This function makes it possible to perform nanoscale grasping without visual feedback (normally in scanning and transmission electron microscopes) in ambient conditions.

Figure 1 shows a schematic diagram of the peeling test of 1D nanostructures with the proposed nanotweezer. Figures 1(a) and 1(b), respectively, show the peeling occurring at the end and in the middle of a 1D nanostructure. For stiff 1D nanostructures, peeling locations can be either at the end or in the middle, whereas for soft 1D nanostructures, notably with a small diameter or a long length, or made up of soft materials, the peeling location is recommended in the middle to avoid sliding off from the nanotweezer during the peeling process. A peeling protocol using the dual-probe nanotweezer can be summarized as follows.

(i) First, testing 1D nanostructures and the end of probe II are accurately located by image scan with probe I by moving the nanostage.

(ii) Once the target 1D nanostructure and peeling locations are determined from the scanned image, the nanotweezer is formed and then approaches to the target peeling location by moving the piezotube and the nanostage alternately.

(iii) Peeling test is started by moving the piezotube on the *Z*-axis when a reliable grasping on the nanostructure is detected with force monitoring. For peeling energy computation, peeling forces are recorded during the whole procedure of the test.

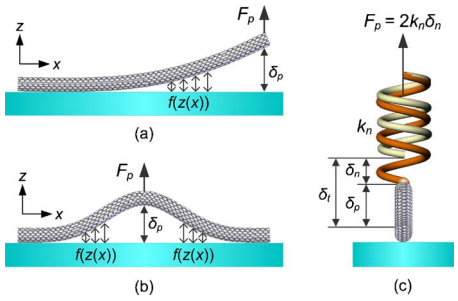

FIG. 2. (Color online) (a) and (b) are, respectively, deflection simulations for peeling locations at the end and in the middle. (c) Peeling force computation model of the peeling test. F_p is the peeling force applied on the peeling location, $f(z(x))$ is the separating gap along the 1D nanostructure, k_n is the stiffness of the cantilever, and δ_n, δ_p, and δ_t are, respectively, the cantilever's normal deflection, the gap on the peeling location, and the displacement on the nanotweezer.

Figures 2(a) and 2(b), respectively, show elastic deformations of a 1D nanostructure when the peeling occurs at the end and in the middle. The gap between the peeling location and the substrate is defined as δ_p, while F_p is the peeling force applied by the nanotweezer at the peeling location. The parameter $z(x)$ describes the gap along the 1D nanostructure from the substrate. As a peeling force computation model shown in Fig. 2(c), F_p can be calculated from the microcantilever's stiffness k_n and deflection δ_n by $F_p=2k_n\delta_n$. In the models, δ_t is the peeling distance on the nanotweezer that can be described as a sum of δ_p and microcantilever's deflection δ_n. In the actual use, δ_p cannot be directly measured. Instead, F_p-δ_t curve during the whole peeling procedure with pickup and release processes is used to estimate the peeling energies.

Figure 3 shows a mechanics analysis of a nanotweezer probe during a peeling operation. Forces applied on the probe tip can be resolved into two components on the *X*- and *Z*-axes in the defined frame, i.e., F_x and F_z, respectively. F_x is the clamping force that holds the 1D nanostructure and F_z

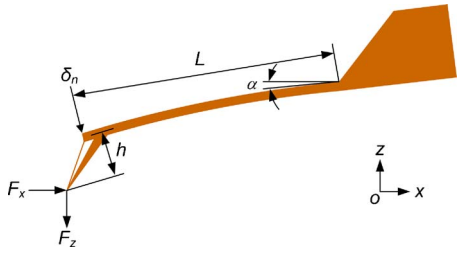

FIG. 3. (Color online) Analysis of mechanics of the nanotweezer probe (a cantilever with beam length L, mounting angle α, and tip height h) during a peeling test. A normal deflection δ_n on a microcantilever is caused by both the clamping force F_x and the peeling force F_z applied at the end of the tip.

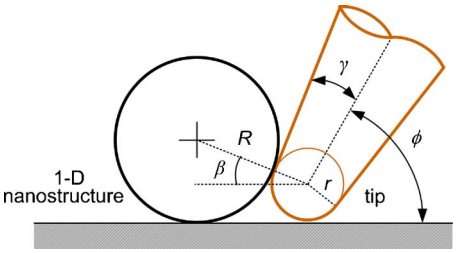

FIG. 4. (Color online) A schematic diagram of a geometry simulation of grasping limit on the size of the 1D nanostructure. ϕ and γ are, respectively, the tip's titled angle relative to the substrate and half-cone angle, R and r are, respectively, radii of 1D nanostructure and the tip apex, and β is defined as the contact angle between the tip apex and the 1D nanostructure.

is the peeling force that balances adhesion forces from the substrate. To sense the peeling force, it is necessary to detect the normal deflection δ_n on each cantilever. δ_n can be calculated by

$$\delta_n = \frac{F_z \cos\alpha + F_x \sin\alpha}{k_n} + \frac{F_z \sin\alpha + F_x \cos\alpha}{k_{xz}}, \quad (1)$$

where $\alpha=5°$ is the mounting angle of the cantilever, $k_{xz}=2lk_n/3h$ is the bending stiffness due to the moment applied on the tip end, here, h is the tip height, and L is the beam length of the cantilever. Assuming that the magnitudes of F_z and F_x are of the same order, contributions from F_x to δ_n can be ignored since it is very small compared with that of F_z due to $k_{xz} \gg k_n$ with $L=250$ μm and $h=15$ μm. Thus, only F_z is considered for the normal deflection δ_n calculation, which can be estimated from the normal voltage output ΔV_n of the optical levers by

$$F_z = C_n \Delta V_n, \quad (2)$$

where C_n is the normal force convention factor of the optical lever. The peeling force F_p can be synthesized from bending forces F_{z1} and F_{z2} that are estimated from the voltage outputs ΔV_{n1} and ΔV_{n2}, respectively, on tips I and II

$$F_p = F_{z1} + F_{z2} = C_{n1}\Delta V_{n1} + C_{n2}\Delta V_{n2}. \quad (3)$$

However, like other manipulation tools, the dual-probe nanotweezer has its own grasping limit on the diameter of 1D nanostructures. The minimum diameter that can be peeled is generally determined by the size of the tip apex and tips' deformations during peeling. The effects from the deformations can be counteracted by preloading a clamping force F_x. Thus, the size of the tip apex is the determinative factor. A geometric simulation of the grasping limit is seen at the bottom inset of Fig. 4, in which $\phi=60°$ is the tip's tilted angle through its rotation axis relative to the substrate; $\gamma=8°$ is the half-cone angle of the tip; $r=8$ nm and R are, respectively, the radii of the tip apex and the 1D nanostructure. The grasping limit $R_{\min}$ can be theoretically equal to r with a proper clamping force. However, grasping will become loose when R decreases below the point where the contact is between the tip apex and the 1D nanostructure (sphere-sphere contact with a smaller contact angle β). Thus, from the relation,

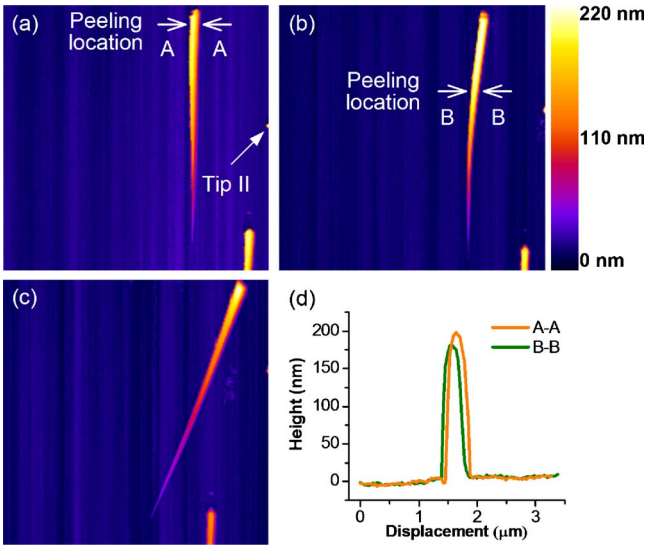

FIG. 5. (Color online) (a) Prescanned image of SiNWs and the end of tip II. A peeling location is first defined at the end (root) of a selected SiNW. (b) A postpeeling image after 25 peeling tests at the end. Another peeling location is then defined in the middle of the SiNW. (c) A postpeeling image after 20 peeling tests in the middle, in which the peeled SiNW was displaced due to complicated interactions among the nanotweezer, the SiNW, and the substrate. (d) Line scans show heights of the peeling locations at the end (196 nm) and in the middle of the SiNW (145 nm).

$$R = \frac{1+\sin\beta}{1-\sin\beta} r, \quad (4)$$

where $\beta_{\max}=90°-\phi-\gamma=22°$, a grasping limit $D_{\min}=2R_{\min}=35.2$ nm can be calculated. It can be found that a wide range of peeling sizes from the nanoscale to the scale of several micrometers can be expected.[25]

III. RESULTS AND DISCUSSION

Peeling tests of a silicon nanowire (SiNW) have been processed with the proposed nanotweezer in an ambient temperature of 20 °C and a relative humidity of 40%. As seen in Fig. 5(a), the cone-shaped SiNWs, with a diameter of 25 nm (top) ~200 nm (root) and a length of about 7 μm, were deposited on a silicon substrate (with 300 nm silicon dioxide) for peeling tests. Once the SiNW was clamped, the peeling was started by moving the piezotube down while nanotweezer kept immovable, followed by a retraction for releasing as the SiNW was completely peeled from the substrate. The tests were repeated dozens of times. Figure 5(b) shows a postpeeling image after 25 tests at the end. Then 20 tests were performed in the middle of the SiNW. As seen in the postpeeling image [Fig. 5(c)], the peeled SiNW was displaced due to complicated interactions among the SiNW, nanotweezer, and the substrate. Figure 5(d) shows heights at peeling locations: 196 nm at the end and 145 nm in the middle of the SiNW.

Figure 6(a) shows a full peeling force spectroscopy curve for the peeling point at the end of the SiNW. When the peeling begins, the peeling force F_p decreases rapidly. At $\delta_t=-115$ nm, the nanotweezer pulls off the substrate. Further peeling leads to four local increases in the force magnitude that are followed, respectively, by discontinuous jumps

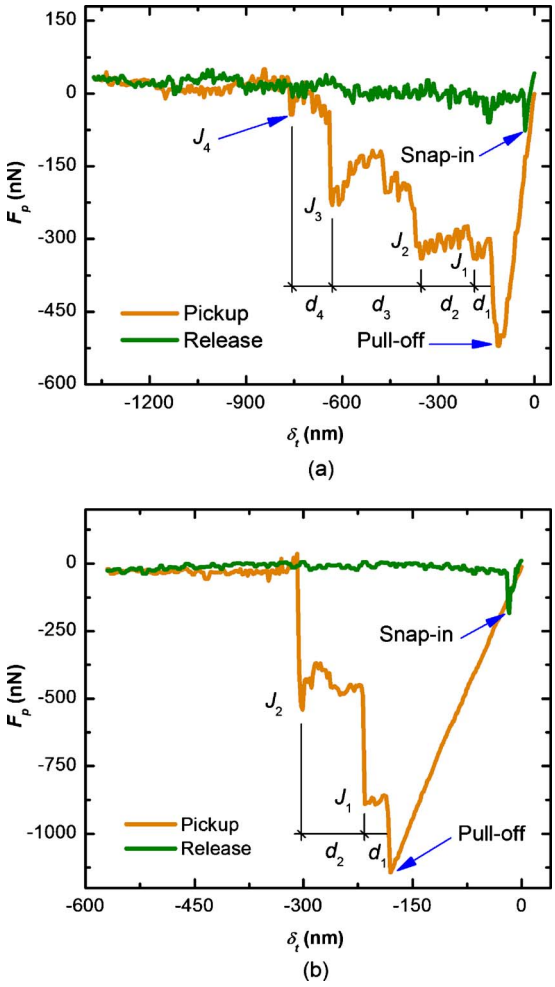

FIG. 6. (Color online) A full peeling force spectroscopy curve recorded by peeling the end of the SiNW. (b) A full peeling force spectroscopy curve recorded by peeling the middle of the SiNW.

J_1-J_4, respectively, with distances d_1-d_4. At $\delta_t=-755$ nm, the peeling force jumped to zero. Upon still further moving substrate down, the peeling force remains zero, indicating that the SiNW has been fully peeled from the surface. During the retraction, neither the nanotweezer nor the SiNW interacts with the approaching surface and the force on the nanotweezer remains around zero. Eventually, the nanotweezer snaps into the substrate at the location close to the starting point. Figure 6(b) shows a full peeling force spectroscopy curve when the peeling location is in the middle of the SiNW. A shorter peeling distance and only two distinct jumps are observed, which is attributed to double peeling interfaces in this case, and reasonably, larger peeling force is obtained. From records of the 25 peeling tests at the end, an average value of the adhesion energies of 1185 keV is calculated. An adhesion energy of 906 keV in the middle is averaged from the 20 peeling tests, which is slightly smaller than the peeling energy at the end. The results are reasonable since the peeling in the middle needs stronger clamping force before peeling that might already break a small part of adhesion at the peeling location.

In summary, we have presented a method for *in situ* peeling test of 1D nanostructures. This method uses a dual-probe nanotweezer that has capabilities of pick-and-place the 1D structures as well as accurate force sensing during the manipulation. With this method, a 1D nanostructure can be easily peeled from the surface by grasping it at various locations without complicated sample preparation. Experimental results of SiNW peeling tests on a silicon surface validate the proposed method. Moreover, peeling applications of the dual-probe nanotweezer could be used to peel other types of nanostructures, e.g., zero-dimensional nanoparticles and three-dimensional nanostructures. In addition, peeling applications of the dual-probe nanotweezer can be extended from the nanoscale to the scale of several micrometers.

ACKNOWLEDGMENTS

This work has been partly supported by the French National Agency of Research through the NANOROL project under Grant No. PSIROB07-184846.

[1] A. H. Barber, S. R. Cohen, and H. D. Wagner, Appl. Phys. Lett. **82**, 4140 (2003).
[2] O. Breuer and U. Sungararaj, Polym. Compos. **25**, 630 (2004).
[3] M. C. Strus, C. I. Cano, R. B. Pipes, C. V. Nguyen, and A. Raman, Compos. Sci. Technol. **69**, 1580 (2009).
[4] M. J. Sever, J. T. Weisser, J. Monahan, S. Srinivasan, and J. J. Wilker, Angew. Chem., Int. Ed. **43**, 448 (2004).
[5] X. Shi, Y. Kong, Y. Zhao, and H. Gao, Acta Mech. Sin. **21**, 249 (2005).
[6] L. Ge, S. Sethi, L. Ci, P. M. Ajayan, and A. Dhinojwala, Proc. Natl. Acad. Sci. U.S.A. **104**, 10792 (2007).
[7] J. E. Jang, S. N. Cha, Y. Choi, G. A. J. Amaratunga, D. J. Kang, D. G. Hasko, J. E. Jung, and J. M. Kim, Appl. Phys. Lett. **87**, 163114 (2005).
[8] E. Dujardin, V. Derycke, M. F. Goffman, R. Lefèvre, and J. P. Bourgoin, Appl. Phys. Lett. **87**, 193107 (2005).
[9] S. N. Cha, J. E. Jang, Y. Choi, G. A. J. Amaratungab, D. J. Kang, D. G. Hasko, J. E. Jung, and J. M. Kim, Appl. Phys. Lett. **86**, 083105 (2005).
[10] K. L. Ekinci and M. L. Roukes, Rev. Sci. Instrum. **76**, 061101 (2005).
[11] B. Mahar, C. Laslau, R. Yip, and Y. Sun, IEEE Sens. J. **7**, 266 (2007).
[12] M. Dragoman, A. Takacs, A. A. Muller, H. Hartnagel, R. Plana, K. Grenier, and D. Dubuc, Appl. Phys. Lett. **90**, 113102 (2007).
[13] Q. Li, S. M. Koo, C. A. Richter, M. D. Edelstein, J. E. Bonevich, J. J. Kopanski, J. S. Suehle, and E. M. Vogel, IEEE Trans. Nanotechnol. **6**, 256 (2007).
[14] I. Popov, S. Gemming, S. Okano, N. Ranjan, and G. Seifert, Nano Lett. **8**, 4093 (2008).
[15] M. Sitti and H. Hashimoto, IEEE/ASME Trans. Mechatron. **5**, 199 (2000).
[16] L. Tong, T. Zhu, and Z. Liu, Appl. Phys. Lett. **92**, 023109 (2008).
[17] C. H. Shin, I. S. Jeon, S. H. Jeon, and Z. G. Khim, Appl. Phys. Lett. **94**, 163107 (2009).
[18] Y. Ishii, A. Ishijima, and T. Yanagida, Trends Biotechnol. **19**, 211 (2001).
[19] M. R. Falvo, R. M. Taylor II, A. Helser, V. Chi, F. P. Brooks, Jr., S. Washburn, and R. Superfine, Nature (London) **397**, 236 (1999).
[20] E. Tranvouez, E. Boer-Duchemin, G. Comtet, and G. Dujardin, Rev. Sci. Instrum. **78**, 115103 (2007).
[21] M. C. Strus, L. Zalamea, A. Raman, R. B. Pipes, C. V. Nguyen, and E. A. Stach, Nano Lett. **8**, 544 (2008).
[22] M. Ishikawa, R. Harada, N. Sasaki, and K. Miura, Appl. Phys. Lett. **93**, 083122 (2008).
[23] H. Xie, D. S. Haliyo, and S. Régnier, Appl. Phys. Lett. **94**, 153106 (2009).
[24] H. Xie, M. Rakotondrabe, and S. Régnier, Rev. Sci. Instrum. **80**, 046102 (2009).
[25] H. Xie and S. Régnier, J. Micromech. Microeng. **19**, 075009 (2009).